7

Self-Organization of Mesoscopically-Ordered Parallel Rare-Eath Silicide Nanowire Arrays on Si(110)-16×2 Surface

Ie-Hong Hong
Department of Electrophysics, National Chiayi University, Chiayi, Taiwan

1. Introduction

One-dimensional nanowires have attracted significant attention due to their exotic physical properties and potential applications in nanoelectronic, nanophotonic, molecular-electronic, and magnetoelectronic devices (Agarawal, 2008; Gambardella *et al.*, 2002; Melosh *et al.*, 2003; Segovia *et al.*, 1999; Snijders, & Weitering, 2010; Yeom *et al.*, 2005; Zeng *et al.*, 2008). In particular, rare-earth metal silicide nanowires are excellent candidates as low-resistance interconnections or as fully-silicided nanoelectrodes for attaching electrically active nanostructures within a nanodevice because of their high conductivity and extremely low Schottky barrier height on *n*-type silicon and their compatibility with current silicon-based integrated circuit technology. As the continuing miniaturization encounters the lithographical limits, self-assembly (Shchukin & Bimberg, 1999) is being regarded as an effective bottom-up approach for growing one-dimensional nanowires because of its potential advantages of low cost, simplicity and high throughput. Moreover, it is believed that the basic building blocks for future complementary metal-oxide-semiconductor (CMOS) architectures will feature the integration of nanostructures based on self-assembly (Lu & Lieber, 2007; Zhirnov & Herr, 2001). In this regard, the self-assembly of epitaxial rare-earth silicide nanowires on silicon surfaces is the subject of numerous studies. It has been shown that Gd, Dy, Er, Y, and Ho can self-assemble into epitaxial silicide nanowires on a planar Si(001)-2×1 surface with large aspect ratios (length > 1 μm, width < 10 nm) by utilizing the anisotropic lattice mismatch between the rare-earth metal silicides and the Si substrate; these rare-earth silicide nanowires grow to arbitrary length in the direction of small (<1%) mismatch and are limited in the lateral direction of large (~8%) mismatch (Chen *et al.*, 2000, 2002; Iancu *et al.*, 2009; Lee & Kim, 2003; Liu & Nogami, 2003a; Nogami *et al.*, 2001; Ohbuchi & Nogami, 2006; Ye *et al.*, 2009; Zeng *et al.*, 2008; Zhang *et al.*, 2009; Zhou *et al.*, 2006).

However, due to the alternating domains of 2×1 and 1×2 reconstruction on the neighboring single-height atomic terraces of the nominally flat Si(001) surface, rare-earth silicide nanowire always grow in two orthogonal directions on the planar Si(001) substrate. These silicide nanowires formed with two perpendicular orientations will intercept each another to terminate further growth of these orthogonal nanowires. Consequently, it is difficult to obtain parallel-aligned and long nanowires for the application in nanoelectronic devices. Therefore, several studies have attempted to use a single-domain vicinal Si(001) surface as a

template to grow a large array of unidirectional rare-earth silicide nanowires (Lee *et al*., 2006; Liu & Nogami, 2003b; Preinesberger, 2005 ; Yeom *et al*., 2005). Although a massively parallel array of straightly-aligned nanowires can be produced by such an approach, the resulting nanowires are randomly-distributed, and different in size. Even an attempt to use a highly-anisotropic vicinal Si(557) surface as a nanotemplate fails to self-organize a highly-regular parallel rare-earth silicide nanowire array over mesoscopic areas of Si(557) surface (Wanke *et al*., 2008). For practical applications of rare-earth silicide nanowires in nanoelectronic architectures, it is of paramount importance to self-organize a massively periodic array of parallel-aligned silicide nanowires with uniform distribution, single orientation and identical size over a macroscopic area on silicon surfaces.

We have recently demonstrated that the most straightforward bottom-up approach for growing a well-ordered, highly-integrated two-dimensional networks and one-dimensional parallel arrays is to use a Si(110)–16×2 surface as a nanopatterned template (Hong *et al*., 2009a, 2009b, 2011a, 2011b, 2011c). Because the 16×2 reconstruction consists of a unique periodic up-and-down sequence of terraces with a perfect periodicity of 5 nm and an equal width of 2.5 nm (An *et al*., 2000), this naturally-patterned nanotemplate is thus very promising for the self-ordered growth of extremely-regular parallel nanowire arrays with high nanowire density and good uniformity over mesoscopic areas. Moreover, Si(110) wafer has been recognized as an ideal substrate for next-generation CMOS nanodevices (Yang *et al*., 2006; Mizuno *et al*., 2005), because CMOS transistors fabricated on Si(110) wafers exhibit both higher hole mobility and ultra-dense spatial integration than ones fabricated on Si(100) wafers (Cheng *et al*., 2006). Thus, a larger-area self-organization of highly-integrated, well-regular, parallel epitaxial nanowire arrays on Si(110) surface can provide an efficient wafer-scale integration for the construction of future nanowire-based CMOS nanodevices.

In this chapter, we present that a large-scale self-organization of highly-regular, parallel arrays of epitaxial rare-earth metal silicide nanowires, covering a mesoscopic area exceeding 1×1 μm², can be realized through the heteroepitaxial growth of rare-earth metal silicides along the periodic terraces of a Si(110)-16×2 surface. Here, we chose Gd, Ce and Er metals to self-form massively highly-ordered rare-earth silicide nanowire arrays on Si(110)-16×2 surface, based on the following reasons: (1) The half-filled *4f* electronic state of Gd atom contains seven spin-up electrons, Gd atoms can act as a source of spin-polarized electrons injected into silicon and create spin chains via the magnetic coupling between the large magnetic moments of *4f* electrons in the adjacent atomic chaisn (McChesney *et al*.,; Žutić, 2006). Also, $GdSi_{1.7}$ epilayers exhibit magnetic ordering below 44 K (Hogg *et al*., 2002) and $Gd_5(Si_{1-x}Ge_x)_4$ has a giant magnetoresistance within the range from 270 K to 290 K (Pecharsky & Gschneidner, 2001). (2) $CeSi_x$ (where $1.0 \leq x \leq 2.0$) compounds have been reported to have many intriguing physical properties, such as intermediate valence, Kondo lattice, heavy-fermion superconductivity and giant magnetoresistance (Münzenberg *et al*., 2007; Shaheen & Mendoza, 1999; Smith *et al*., 2005; Yokota *et al*., 2002); however, so far no Ce-silicide nanowires can be formed by using the anisotropic lattice-mismatched growth because of the poor lattice mismatches between silicides of the light rare-earth metal Ce and Si(001) substrate along two orthogonal crystalline directions. (3) Er silicides not only possess the lowest resistance of all rare earth metal silicides, but also exhibit anomalous Hall effect below 60 K (Pierre *et al*., 1994) and present strong magnetic dichroism due to the large magnetocrystalline anisotropy at room temperature (Castrucci *et al*., 1995).

Our results demonstrate the fact that our developed template-directed self-organization process based on the nanotemplate of Si(110)-16×2 superstructure can be applicable for the

spontaneous formation of massively well-regular parallel arrays of other epitaxial rare-earth metal silicide nanowires, and open up the possibility for self-ordered, large-area, parallel arrays of magnetic atomically-precise rare-earth metal silicide nanowires on Si(110)–16×2 surface, which could be integrated into high-density magnetoelectronic or spintronic nanodevices. Moreover, the excellent regularity of our fabricated well-ordered parallel rare-earth silicide nanowire arrays is comparable to that fabricated lithographically (Melosh *et al.*, 2003), and is much better than that produced by the anisotropic lattice mismatch growth. This advantage allows us to further carry out detailed investigations of electronic, chemical and magnetic properties of such massive self-ordered parallel rare-earth silicide nanowire arrays by means of photoemission spectroscopy (Segovia *et al.*, 1999; Yeom *et al.*, 2005) and magnetic circular dichroism (Gambardella *et al.*, 2002).

2. Experimental methods

The experiments were performed in a commercial, ultrahigh vacuum, variable-temperature STM system with a base pressure of ~5×10^{-11} mbar. The device-quality flat Si(110) substrates (n-type, ~10 Ωcm) were used as one-dimensional nanotemplates for the self-organization of parallel rare-earth silicide nanowire arrays. Atomically clean Si(110)-16×2 surface was prepared by well-established annealing procedures (Hong *et al.*, 2009a, 2009b), and was confirmed by STM observation of the long-range 16×2 superstructure, as shown in Fig. 1. Parallel Gd-silicide nanowire arrays were produced by depositing ~6 Å of high purity (99.95%) Gd onto Si(110) surface at 750 ^{o}C at a deposition rate of ~0.1 Å/min and subsequently quenching to room temperature. Parallel Ce-silicide nanowire arrays were produced by depositing ~8 Å of high-purity (99.95%) Ce metals onto Si(110) surface at 400 ^{o}C at a deposition rate of ~0.2 Å/min and subsequently annealing at 700 ^{o}C for 20 minutes, then slowly cooling down to room temperature. Parallel Er-silicide nanowire arrays were produced by depositing ~10 Å of high-purity (99.95%) Er metals onto Si(110) surface at 650 ^{o}C at a deposition rate of ~0.2 Å/min and subsequently annealing at 750 ^{o}C for 30 minutes. Gd, Ce and Er metals were evaporated individually from a water-cooled electron-beam evaporator with an internal flux meter; their deposition coverages were determined *in situ* using a quartz-crystal thickness monitor. During the deposition of these rare-earth metals, the system pressure was maintained below 1×10^{-9} mbar. The STM measurements were acquired in the constant current mode with the atomic-resolution electrochemically etched nickel tips. The I-V curve was performed by recording the tunneling current (I_t) while ramping the sample bias (V_s) at a specific location on the nanowire; and was then numerically differentiated to obtain the dI/dV curve (i.e., STS spectrum).

3. Results and discussion

3.1 One-dimensional naturally-patterned nanotemplate of Si(110)-16×2 surface

3.1.1 Atomically clean Si(110)-16×2 surface

Figure 1 represents typical STM topographic images of the atomically clean Si(110)–16×2 surface at different magnifications. As visibly seen in Figs. 1(a) and 1(b), the parallel-aligned up-and-down terraces of the 16×2 superstructure extending over a wide area exhibit a mesoscopic ordering and clearly reveal a unique highly-anisotropic character of this reconstruction. Such uniform grating-like terraces are very suitable to be used as a novel

nanotemplate for the large-scale nanofabrication of well-ordered, high-density, parallel-aligned nanowires covering macroscopic areas. A magnified image (50 × 50 nm²) of a part of Fig. 1(b) is shown in Fig. 1(c). It obviously shows that zigzag chains appear in the grating-like up-and-down terraces. An atomic-resolution image (12 × 12 nm²) of Fig. 1(d), magnified from Fig. 1(c), shows a pair of Si pentagons forming zigzag chains on the upper terraces of 16×2 reconstruction are clearly resolved, consistent with the pervious result (An *et al.*, 2001; Stekolnikov *et al.*, 2004). Figure 2 displays the cross-sectional profile across the up-and-down terraces of 16×2 reconstruction along the line scans **C** in Fig. 1(c). The typical width and average height of these periodic upper terraces are 2.2 ± 0.1 nm and 0.29 ± 0.01 nm, respectively, and the regular periodicity is 5.0 ± 0.1 nm. These measurements are consistent with the previous results (An *et al.*, 2001; Yamamoto *et al.*, 2000).

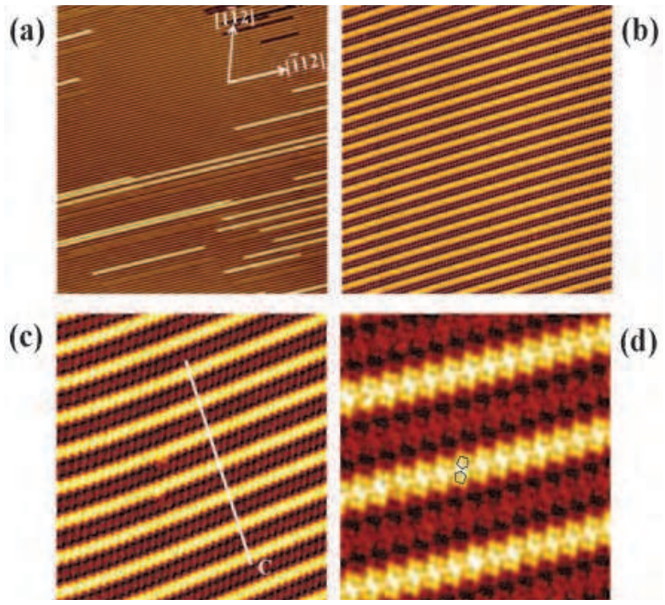

Fig. 1. (a)−(c) STM topographic images of the atomically clean Si(110)-16×2 surface taken at different magnifications: (a) 500 × 500 nm² (V_s = +3 V, I_t = 30 pA), (b) 125 × 125 nm², (c) 50 × 50 nm², and (c) 15 × 15 nm² (V_s = +1.5 V and I_t = 10 pA).

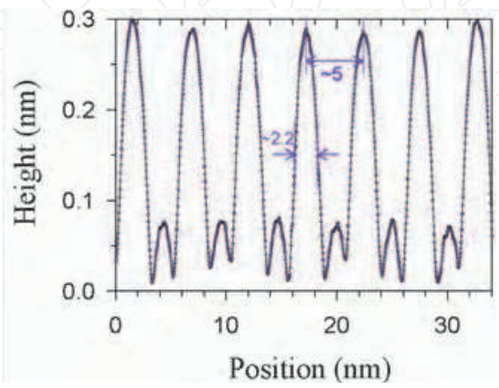

Fig. 2. Cross-sectional profile across the up-and-down terraces of 16×2 reconstruction along the white line indicated in Fig. 1(c).

3.1.2 Parallel silicon nanowire array grown naturally on Si(110) surface

Since both the width and height of these upper terraces of Si(110)–16×2 surface are nearly close to those of silicon nanowires formed on Ag(110) surface (Sahaf *et al.*, 2007; Padova *et al.*, 2008), the long-range, parallel-aligned upper terraces of 16×2 reconstruction can be recognized as massively-parallel silicon nanowires grown naturally on Si(110) surface. The identification of the upper Si(110) terraces as silicon nanowires formed on Si(110) surface is similar to the self-formation of massive Si atomic lines on the Si-terminated β-SiC(100)-3×2 surface (Soukiassian *et al.*, 1997). Silicon nanowires has been regarded as the most promising basic building blocks for the bottom-up assembly of integrated electronic and photonic nanodevices because they have the advantage of easy integration into the existing silicon-based semiconductor industry (Agarawal, 2008; Lu & Lieber, 2007).

3.2 Parallel Gd-silicide nanowire array self-organized on Si(110)-16×2 surface

Figures 3(a)−3(e) show the representative STM topographic images of parallel Gd-silicide nanowire array at different magnifications. As clearly observed in Figs. 3(a)−3(e), these parallel-aligned, straight and nearly defect-free nanowires cover a mesoscopic area with a typical lateral separation beyond 1.0 μm and are most elongated along the $[\bar{1}\ 1\ 2]$ direction. In Fig. 3(d), each Gd-silicide nanowire consists of double bead chains separated by a bean chain. The double bead chains are higher than the bean chain by a difference of ~25 pm, as shown in the cross-sectional profile of Fig. 4. Each bead chain is composed of rounded protrusions marked by the red circles of ~1.5 nm in diameter, which are too large to be interpreted as individual atoms. Additionally, the adjacent substrate between the neighboring nanowires still shows a zigzag chain structure. All individual nanowires are atomically precise nanostructures, essentially identical to one another over the entire macroscopic area of Si(110) surface. Their width remains atomically precise along the nanowire and is typically 4.0 ± 0.1 nm [see Fig. 4]. Therefore, these nanowires possess an extraordinarily high aspect ratio of greater than 250. Moreover, this massively parallel array shows a regular periodicity of 7.2 ± 0.2 nm [see Fig. 4]. Such a perfect one-dimensional self-organized parallel nanowire array with good uniformity and alignment over a mesoscopic area represents a well-established long-range spatial ordering. This large-area Gd-silicide nanowire array also exhibits a high nanowire density and thus can be applied for the wafer-scale integration of high-density nanoelectronic devices. The growth mechanism of such a highly-regular parallel array of uniformly-spaced Gd-silicide nanowires on Si(110)-16×2 surface is driven by the heteroepitaxial growth of Gd silicides on these periodic grating-like upper terraces of Si(110)-16×2 superstructure, as explained in detail in our previous publication (Hong *et al.*, 2009a). This perfect self-organization of a large-area parallel array consisting of atomically-precise Gd-silicide nanowires with regular periodicity is observed for the first time.

Figures 3(e) and 3(f) show an enlarged part of the STM image in Fig. 3(d), recorded at the sample bias V_s = +2.0 V and −2.0 V, respectively. We note that both empty-state and filled-state STM images [i.e., Figs. 3(e) and 3(f)] represent the same area of the sample. In dual-bias images, the parallel, registry-aligned nanowires are well resolved. The empty-state image [Fig. 3(e)] clearly shows that the rounded protrusions of the double bead chains in Fig. 3(d) converts to pentagons; however, the pentagons in the left and right bead chains are oppositely oriented, which is the same as the pair of Si pentagons of Si(110)-16×2 superstructure [see Fig. 1(d)]. Moreover, the bean chain disappears and instead becomes to a

trench. This result strongly suggests that the Si pentagon pair on the upper terraces of 16×2 reconstruction was split into two individual Si pentagons due to a strong reaction of Si and Gd upon the adsorption of Gd on the upper terraces. Consequently, a trench was formed in the middle of Gd-silicide nanowires and Gd atoms were embedded in the trench (i.e., Gd atoms were adsorbed in the bean chain of Fig. 3(d)), similar to the Si-deficient structural model (Lee & Kim, 2003). The width of Gd-silicide nanowire thus becomes to be ~4 nm from the Si terrace width of ~2.2 nm. In the filled-state image [Fig. 3(f)], each Gd-silicide nanowire appears to consist of two sawtooth rows of distinct atomic arrangements on both sides and a pair of double linear chains with an up-down buckling configuration in the middle of nanowire; moreover, the contrast of these two sawtooth rows is much lower than that of double linear chains. Notice that the dark trench between the double bead chains in Fig. 3(e) inverts to the bright double linear chains in Fig. 3(f) when the bias polarity is reversed. Considering the charge transfer from Si to Gd atoms by electronegativity, the bright double linear chains in Fig. 3(f) are primarily contributed from the electronic states localized on Gd atoms, suggesting that Gd atoms are located on the bean chain in Fig. 3(d). That is, the two sawtooth rows and the double linear atomic chains consist mainly of Si and Gd atoms, respectively. The appearance of the well-ordered internal structures in Gd-silicide nanowires strongly verifies that these straightly-aligned, long Gd-silicide nanowires grow epitaxially on Si(110) surface.

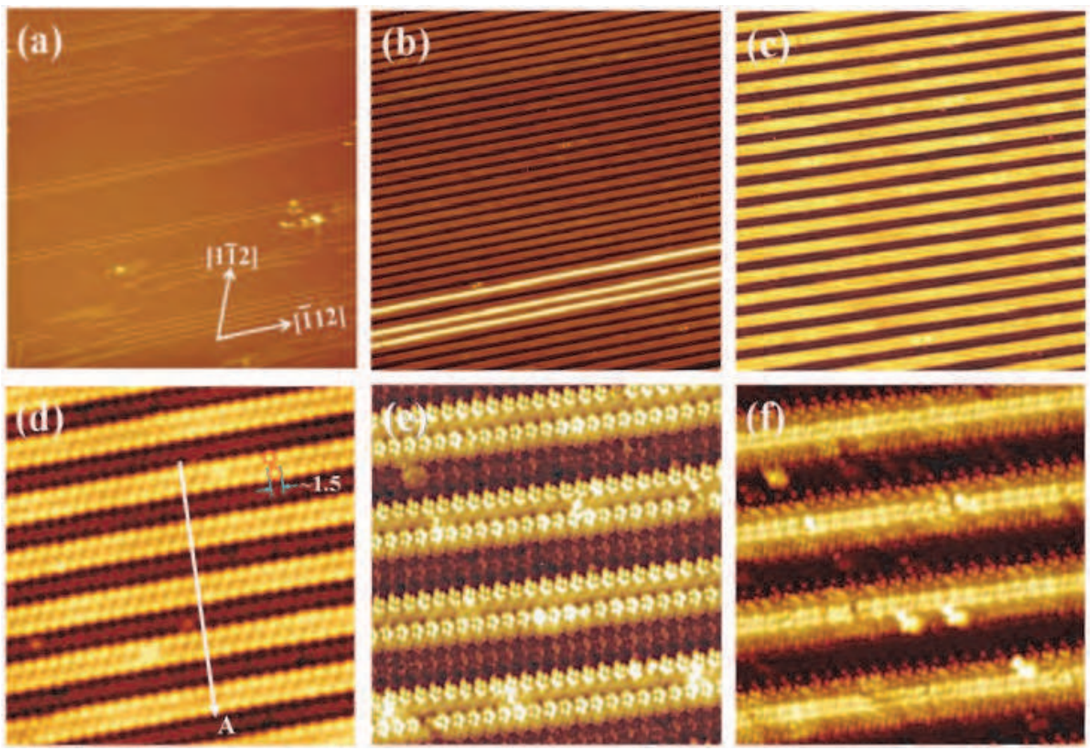

Fig. 3. (a)−(d) STM topographic images of parallel Gd-silicide nanowire array on Si(110)-16×2 surface taken at different magnifications: (a) 0.8 × 0.8 μm² (V_s = +3 V, I_t = 30 pA), (b) 250 × 250 nm², (c) 110 × 110 nm², and (d) 50 × 50 nm². (e), (f) Dual-polarity images (25 × 25 nm²) of parallel Gd-silicide nanowire array acquired at +2 V and −2 V, respectively, and at I_t = 10 pA.

As seen in Figs. 3(e) and 3(f), the two bead chains of empty orbitals on both sides of nanowire are in antiphase with the double linear chains of filled orbitals in the middle of nanowire. This polarity dependence of STM images clearly reveals that each Gd-silicide nanowire really consists of a bundle of chain-like structures with a peculiar charge arrangement of alternating filled and empty orbitals. These dual-polarity STM images clearly show that these parallel-aligned Gd-silicide nanowires are well-defined and periodically arranged in both filled-state and empty-state images. The periodic intensity modulation exhibited by this parallel array in dual-bias images clearly reveals a perfect spatial-organization of the charge distribution. Such a well-regular charge modulation of this parallel Gd-silicide nanowire array could be exploited in nanoelectronic devices.

Figure 4 displays the cross-sectional profiles of the line scan **A** across the parallel Gd-silicide nanowire array in Fig. 3(d). This cross-sectional profiles show clearly that the shape distribution of the parallel Gd-silicide nanowire array is well-defined and uniformly-spaced. The unprecedented uniformity exhibited by this parallel array reflects a perfect spatial-organization characteristic of our performed one-dimensional self-assembling process. As shown in the topographic profile in Fig. 4, the nanowires are typically 4.0 ± 0.1 nm in width and have an average periodicity of 7.2 ± 0.2 nm; the heights observed in the empty-state image and the filled-state image are, respectively, 270 ± 10 pm and 250 ± 10 pm, similar to the height obtained by Lee *et al* (Lee & Kim, 2003). It is noted that the nanowire height is nearly equal to that of Si upper terraces on Si(110)-16×2 surface, which suggests that Gd atoms may incorporate into Si upper terraces to form one-dimensional Gd-silicide nanowires, similar to the proposed structure of Si-deficient rare-earth metal silicide nanowires (Chen *et al.*, 2002; Eames *et al.*, 2010).

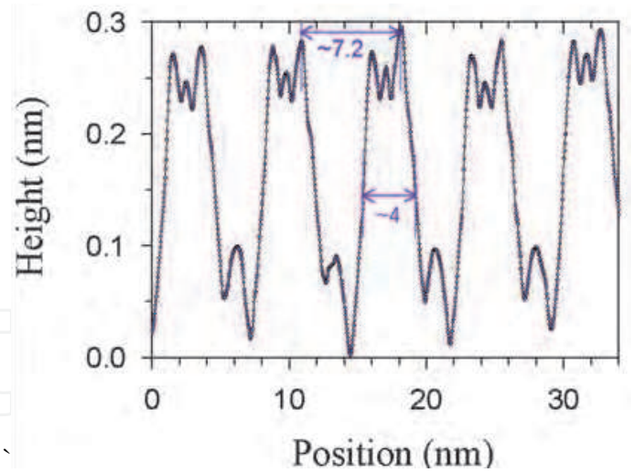

Fig. 4. Cross-sectional profile **A** across the parallel Gd-silicide nanowire array along the white line indicated in Fig. 3(d)

To gain insight into the local electronic structure of Gd-silicide nanowires, STS spectra (i.e., dI/dV curves) were measured on top of the individual Gd-silicide nanowires and the adjacent substrate between neighboring nanowires, as displayed in Fig. 5. A third dI/dV curve taken on clean Si(110) surface is also shown for reference. Each dI/dV curve is laterally averaged over 20 individual spectra taken within the corresponding region. These STS spectra allow us to compare the surface conductivity and local density of states (LDOS)

in the areas selected on the surface. Curve **I** measured on the self-organized parallel Gd-silicide nanowires show non-zero conductance near the zero bias, indicating that Gd-silicide nanowires have one-dimensional metallic character along their length. As clearly revealed in Curve **I**, the Gd-silicide nanowires are characterized by a set of the discrete, distinct electronic states.

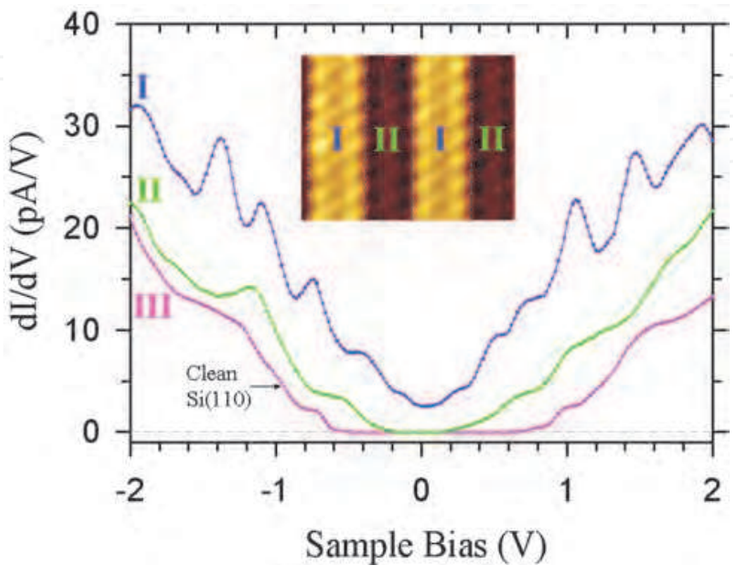

Fig. 5. Averaged dI/dV curves of the parallel Gd-silicide nanowires (Curve **I**), the adjacent substrate (Curve **II**), and the clean Si(110) surface (Curve **III**). Each dI/dV curve was laterally averaged over their corresponding areas in the inserted STM image (15 × 10 nm^2).

These sharp peaks in the STS spectrum of individual Gd-silicide nanowire are characteristic of the Van Hope singularities expected for the LDOS of one-dimensional materials (Iancu *et al.*, 2009; Zeng *et al.*, 2008). Curve **II** taken over the adjacent substrate shows semiconducting behavior with a band gap of ~0.5 eV, significantly smaller than ~1.2 eV for clean Si(110) surface [see Curves **III**]. The reduced gap opening of the substrate together with the zigzag chain structure suggests that Si(110)-16×2 surface is reconstructed with Gd.

3.3 Parallel Ce-silicide nanowire arrays self-organized on Si(110)-16×2 surface

Figure 6 shows the STM topographic images of the parallel Ce-silicide nanowire array at different magnifications. As visibly observed in Figs. 6(a)−6(e), these parallel-aligned, straight and nearly defect-free nanowires cover a mesoscopic area with a typical lateral distance exceeding 1.3 μm and are elongated along the $[\bar{1}\,1\,2]$ direction. These nanowires thus possess an extraordinarily high aspect ratio. Also, this massively parallel nanowire array shows a regular periodicity and a high integration density. Moreover, these parallel nanowires are essentially identical to one another over the entire macroscopic area of the Si(110) surface. This result clearly reveals that these parallel nanowires grew along the periodic terraces of Si(110)-16×2 superstructure. Such large-area parallel Ce-silicide nanowire array could be applied in the wafer-scale integration of high-density nanoelectronic architectures on Si(110) surface. As clearly seen in Fig. 6(e), each Ce-silicide nanowire consists of double zigzag chains with distinct morphologies. In the atomic-

resolution image of Fig. 6(f), we can visibly find that the elemental structures of the double zigzag chains in the Ce-silicide nanowire are completely different from those of up-and-down terraces on Si(110)-16×2 surface; moreover, the width of all individual nanowires remains atomically precise along their lengths. This perfect one-dimensional self-organized parallel array with good uniformity and alignment over a mesoscopic area of 1.3×1.3 μm² reveals a well-established long-range spatial ordering. The spontaneous formation of such a large-area, highly-ordered parallel array consisting of atomically-precise Ce-silicide nanowires with a regular periodicity has never been reported before.

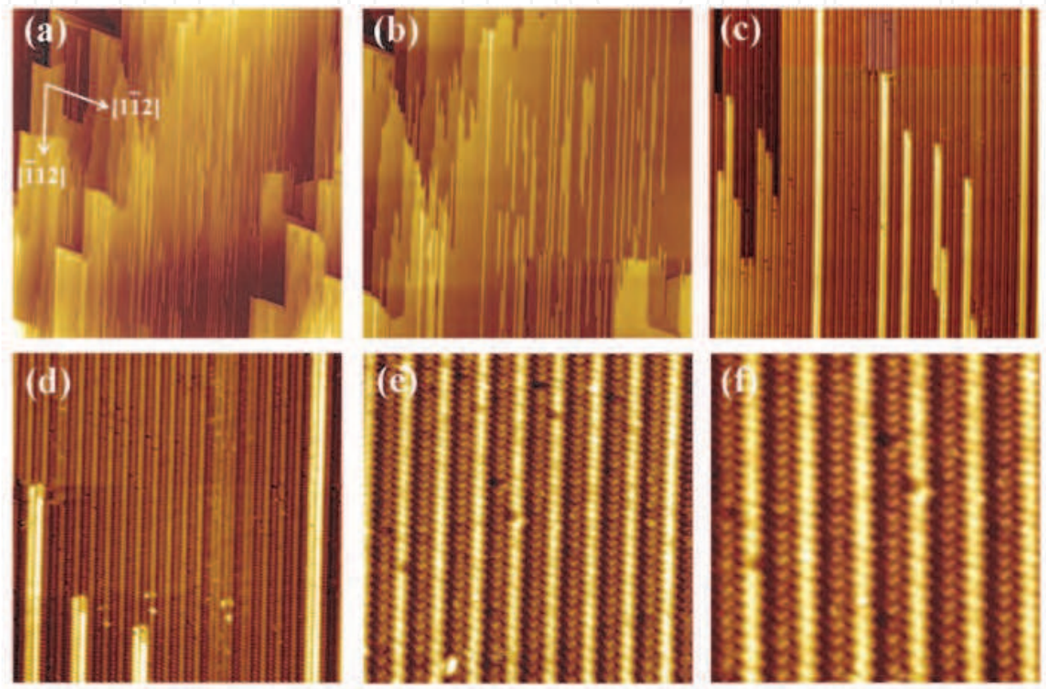

Fig. 6. A series of different magnified STM topographic images of the parallel Ce-silicide nanowire array: (a) 1.3 × 1.3 μm² (V_s = 2.0 V, I_t = 0.1 nA); (b) 850 × 850 nm²; (c) 250 × 250 nm²; (d) 125 × 125 nm²; (e) 50 × 50 nm² (V_s = 2.0 V, I_t = 20 pA); and (f) 35 × 35 nm².

Figures 7(a) and 7(b) show dual-polarity STM images of an enlarged area of the parallel Ce-silicide nanowire array in Fig. 6(e), recorded at the sample bias V_s = +1.5 V and −1.5 V. The empty-state image [Fig. 7(a)] at +1.5 V clearly shows a set of double zigzag chains on each Ce-silicide nanowire and the right zigzag chain appears much brighter than the left chain. In the filled-state image [Fig. 7(b)] at −1.5 V, the Ce-silicide nanowires consist of two linear rows of distinct atomic arrangements and the right linear row is also brighter than the left row. These dual-bias STM images evidently show that Ce-silicide nanowires are registry-aligned and really consist of a bundle of double chain-like structures with different morphologies. Figure 7(c) plots the superposition of the cross-sectional profiles of both line scans **E** and **F** across the empty-state and filled-state images of parallel Ce-silicide nanowires in Figs. 7(a) and 7(b), respectively. The section profiles of both lines **E** and **F** clearly show that these parallel Ce-silicide nanowires are well defined and periodically positioned. The unprecedented regularity exhibited by this parallel array in dual-bias images also reflects a perfect spatial-ordering of the charge distribution.

As clearly revealed in Fig. 7(c), these parallel-aligned nanowires are identical to 5.0 ± 0.2 nm in width and have an equal periodicity of 6.0 ± 0.2 nm. Moreover, the topographic maxima of the double zigzag chains in the empty-state image and the double linear rows in the filled-state image are spatially coincident; indicating that the height difference between the right chains and left chains is due to the topographic effect, not the electronic effect. The left–right asymmetry observed in the dual-polarity images of each Ce-silicide nanowire indicates that the building blocks for Ce-silicide nanowires are asymmetrically composed. Additionally, the widths of the left and right zigzag chains are 2.0 ± 0.2 and 3.0 ± 0.2 nm, respectively; while the double linear rows are equal to 2.5 ± 0.1 nm in width, similar to the width (2.2 ± 0.1 nm) of Si terraces of the Si(110)-16×2 reconstruction [see Fig. 2].

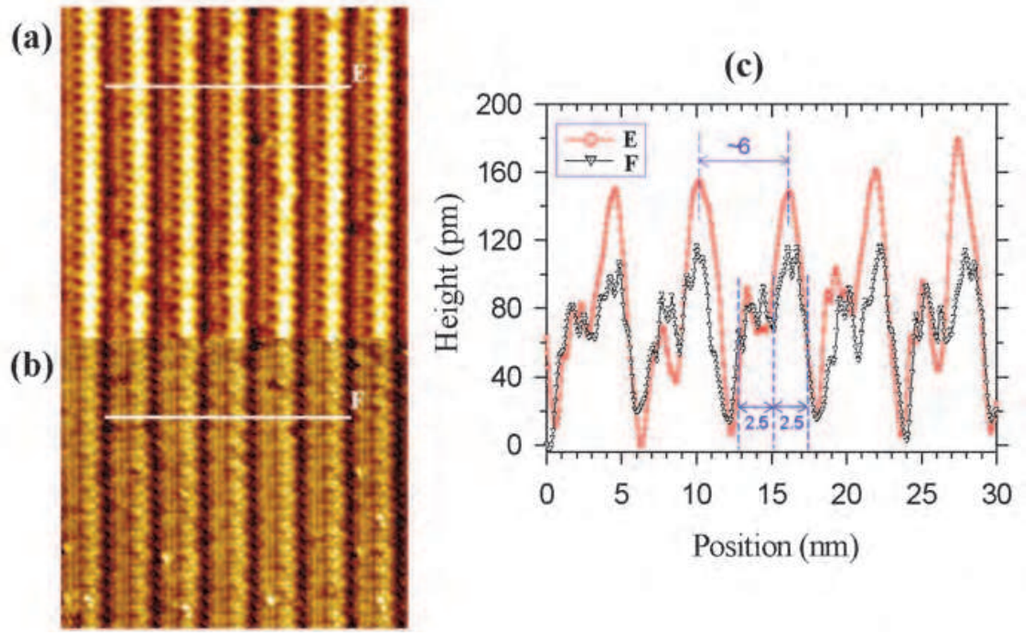

Fig. 7. Dual polarity STM images (45 × 35 nm²) of the parallel Ce-silicide nanowires acquired at +1.5 V (a) and −1.5 V (b), respectively, and at 20 pA. (c) Cross-sectional profiles **E** and **F** across parallel-aligned Ce-silicide nanowires of the empty- and filled-state images along the white lines indicated in (a), respectively.

These results strongly suggest that Ce atoms nucleated concurrently along the upper and lower terraces of Si(110)-16×2 surface to form the one-dimensional Ce-silicide nanowires consisting of double chain row structures with different heights. The Ce-silicide nanowires are characterized by a well-defined shape indicating epitaxial growth, which is promising for the basic building block of nanoelectronic devices.

It is very interesting to explore the local electronic structures of the parallel Ce-silicide nanowire array. STS spectra (i.e., dI/dV curves) were measured on the individual Ce-silicide nanowires and also on the adjacent substrate between the neighboring nanowires, as displayed in Fig. 8. A third dI/dV curve taken on clean Si(110) surface is also shown for comparison. Each dI/dV curve was laterally averaged over 30 individual spectra taken within the corresponding areas indicated in the inserted STM image (20 × 10 nm²). Curve **I** for the left chain shows an energy gap of ~0.68 eV, suggesting a semiconducting property

along its length. These results clearly reveal that self-organized parallel Ce-silicide nanowires are semiconducting. Curve **II** for the adjacent substrate shows a lager energy gap of ~0.9 eV, smaller than the gap of ~1.2 eV obtained for the clean Si(110)-16×2 substrate [see Curve **III**].

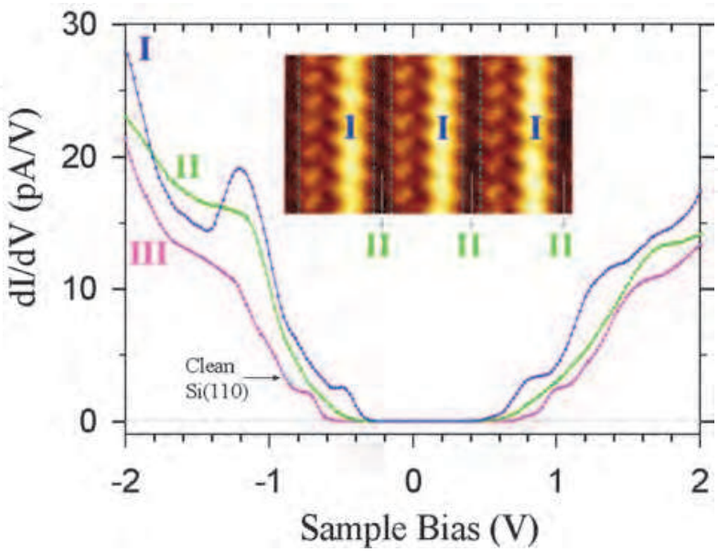

Fig. 8. Averaged STS spectra of the right zigzag chain taken on the individual Ce-silicide nanowires (Curve **I**), the adjacent substrate between neighboring nanowires (Curve **II)**, and the clean Si(110) surface (Curve **III**).

The reduced gap opening of the substrate and the featureless LDOS means that the Si(110) surface was covered with a small amount of Ce. The semiconducting behavior of Ce-silicide nanowires is in contrast to the metallic character of other rare-earth silicide nanowires (Hong *et al.*, 2011a; Lee & Kim, 2003; Yeom *et al.*, 2005; Zeng *et al.*, 2008) and $CeSi_x$ Kondo compounds (Malterre *et al.*, 1993; Mimura *et al.*, 2005). The suppression of LDOS near the Fermi energy (i.e., zero bias) can be ascribed to the formation of a Mott-Hubbard insulating states at these Ce-silicide nanowires (Hong *et al.*, 2011c).

3.4 Parallel Er-silicide nanowire arrays self-organized on Si(110)-16×2 surface

Figure 9 shows a series of different magnified STM topographic images of parallel Er-silicide nanowire arrays. As clearly observed in Fig. 9, these parallel-aligned, straight andnearly defect-free nanowires cover a mesoscopic area with a typical length beyond 1.0 μm and are most elongated along the $[\bar{1}\,1\,2]$ direction. In Fig. 9(e), each Er-silicide nanowire consists of double bead chains, but unlike to the morphology of Gd-silicide nanowire with the bean chain in the middle of nanowire. Each bead chain is composed of round protrusions with a typical diameter of ~2.0 nm. Additionally, the adjacent substrate between the neighboring nanowires still shows a zigzag chain structure. All individual nanowires are atomically precise nanostructures, essentially identical to one another over the entire macroscopic area of Si(110) surface.Their width remains atomically precise along the nanowire and is typically 4.2 ± 0.1 nm [see Fig. 10].Therefore, these nanowires possess an extraordinarily high aspect ratio of greater than 250. Moreover, this massively parallel

array shows a regular periodicity of 8.0 ± 0.2 nm [see Fig. 10]. Such a perfect one-dimensional self-organized parallel nanowire array with good uniformity and alignment over a mesoscopic area represents a well-established long-range spatial ordering. This large-area Er-silicide nanowire array also exhibits a high nanowire density and thus can be applied for the wafer-scale integration of high-density nanoelectronic devices.

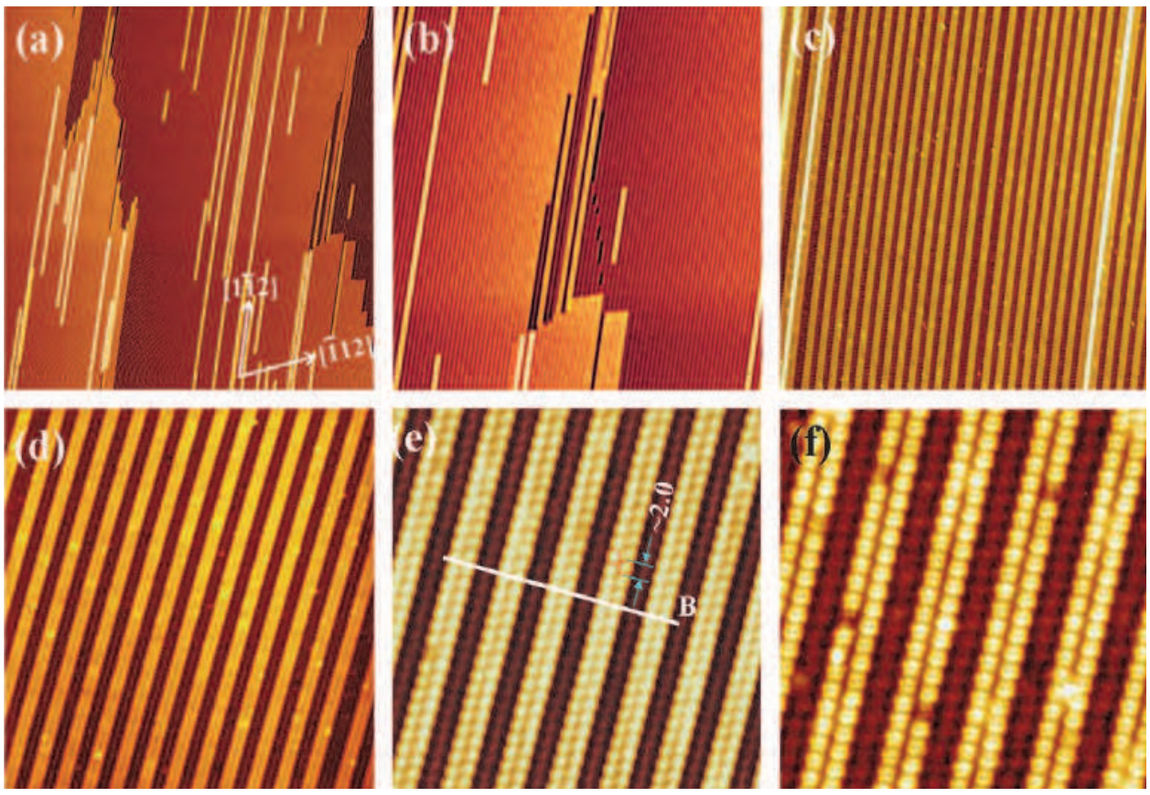

Fig. 9. (a)−(d) STM topographic images of parallel Er-silicide nanowire array on Si(110)-16×2 surface taken at different magnifications: (a) 1 × 1 μm² (V_s = +3 V, I_t = 30 pA), (b) 500 × 500 nm², (c) 200 × 200 nm², (d) 110 × 110 nm², (e) 60 × 60 nm² (V_s = +3 V, I_t = 10 pA), and (f) 36 × 36 nm² (V_s =+2 V, I_t = 10 pA).

Figure 10 displays the cross-sectional profiles of the line scan B across the parallel Er-silicide nanowire array in Fig. 9(e). This cross-sectional profiles show clearly that the shape distribution of the parallel Er-silicide nanowire array is well-defined and uniformly-spaced. The unprecedented uniformity exhibited by this parallel array reflects a perfect spatial-organization characteristic of our performed one-dimensional self-assembling process. As shown in the topographic profile in Fig. 10, the nanowires are typically 4.2 ± 0.1 nm in width and have a representative periodicity of 8.0 ± 0.2 nm; the average heights is 230 ± 20 pm, similar to the height obtained by Chen *et al*. (Chen *et al*., 2002) The growth mechanism of such a highly-regular parallel array of uniformly-spaced Er-silicide nanowires on Si(110)-16×2 surface is also driven by the heteroepitaxial growth of Er silicides along the perfect grating-like upper terraces of Si(110)-16×2 superstructure, similar to the self-organized growth of Gd-silicide nanowires on Si(110)-16×2 surface.

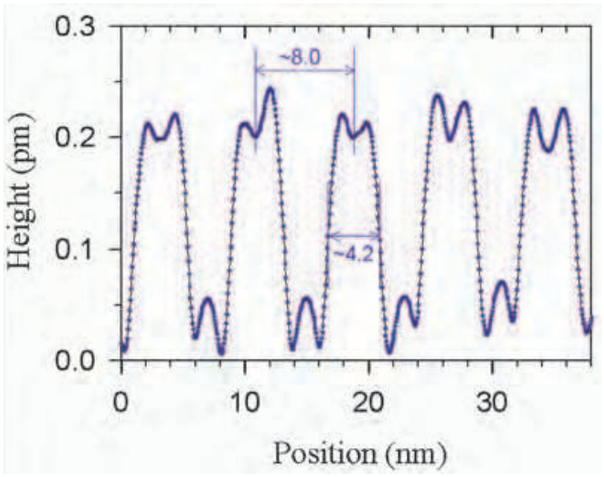

Fig. 10. Cross-sectional profile **B** across the parallel Er-silicide nanowire array along the white line indicated in Fig. 9(e)

Figure 11 displays the representative STS spectra of the self-organized Er-silicide nanowires (Curve **I**) and the adjacent substrate between neighboring nanowires (Curve **II**). Each dI/dV curve is laterally averaged over 30 individual spectra taken within the corresponding region of the inserted STM image. Curves **I** shows non-zero conductance near the zero bias, indicating that Er-silicide nanowires exhibit metallic nature along their length. Curve **II** depicts metallic-like behavior with a narrower band gap of ~0.12 eV, significantly smaller than ~1.2 eV for the clean Si(110) surface [see Curves **III**]. The metallic-like character of the substrate together with the zigzag chain structure suggests that Si(110) surface is reconstructed with Er.

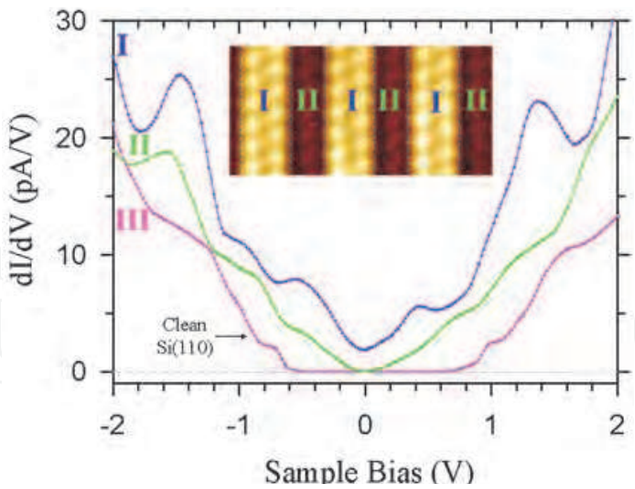

Fig. 11. Averaged dI/dV curves of the parallel Er-silicide nanowires (Curve **I**), the adjacent substrate (Curve **II**), and the clean Si(110) surface (Curve **III**). Each dI/dV curve was laterally averaged over their corresponding areas in the inserted STM image (25× 12 nm^2).

3.5 Parallel transition metal silicide nanowires self-assembled on Si(110)-16×2 surface

As clearly demonstrated in Figs. 3-11, the massively parallel arrays of various epitaxial rare-earth metal silicide nanowires on Si(110)-16×2 surface always grow along a unidirectional

orientation of [$\bar{1}$ 1 2]with uniform distribution and identical size. However, the growth mode of rare-earth metal silicide nanowires on Si(110) surface is completely different from that of the transition-metal silicide nanowires on Si(110) surface. As shown in Fig. 12, the parallel-aligned Ni-silicide and Fe-silicide nanowires can not form well-ordered parallel nanowire arrays with a regular periodicity and identical dimensions on Si(110) surface, as reported in the previous results (He *et al*., 2004; Liang *et al*., 2006). The difference can be attributed to the fact that transition-metal silicide nanowires prefer to grow into the Si(110) substrate along the [$\bar{1}$ 1 0] direction via an "endotaxial" growth mechanism (He *et al*., 2004) and do not favor to nucleate along the [$\bar{1}$ 1 2]-oriented terraces of Si(110)-16×2 reconstruction.

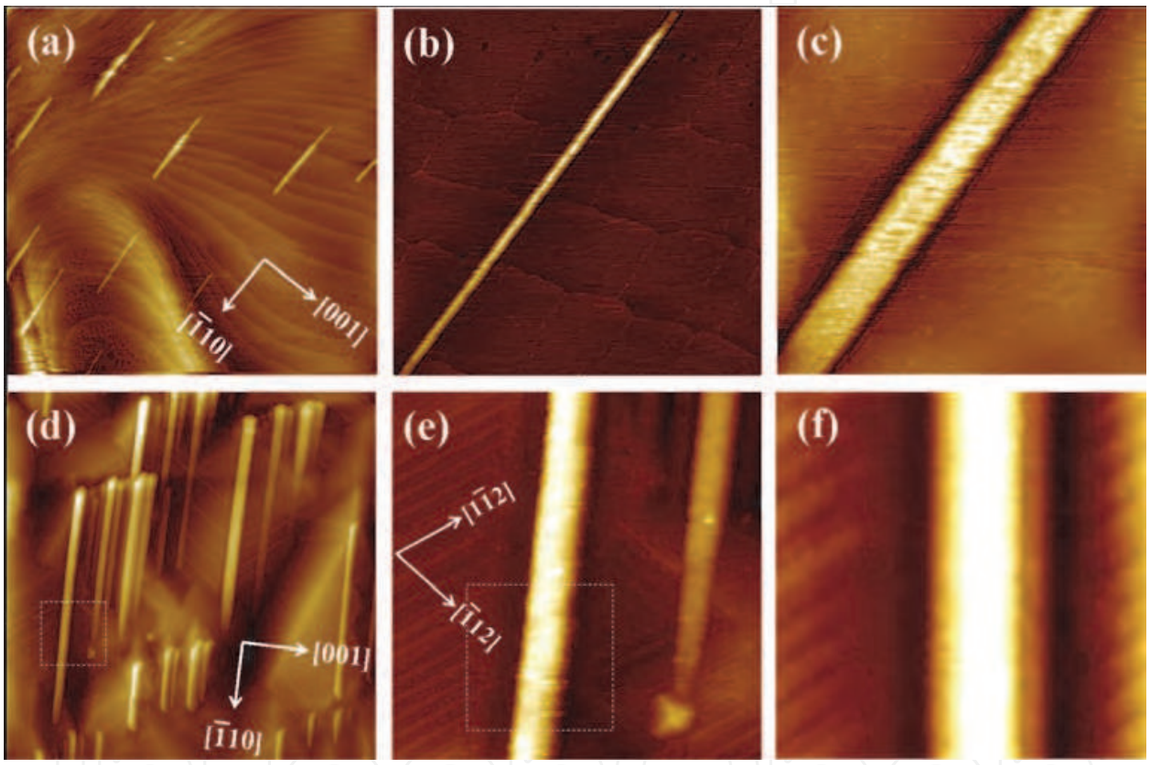

Fig. 12. STM topographic images of parallel Ni-silicide nanowires on Si(110) surface [(a)−(c)] and parallel Fe-silicide nanowires on Si(110) surface [(d)−(f)] at different magnifications: (a) 7 × 7 μm^2, (b) 1× 1 μm^2, (c) 500 × 500 nm^2, (d) 800 × 800 nm^2, (e) 125 × 125 nm^2, and (f) 45 × 45 nm^2.

4. Conclusion

We have successfully developed a simple and efficient bottom-up nanofabrication for the self-organization of mesoscopically-ordered parallel arrays, consisting of uniformly-spaced identical-size epitaxial rare-earth metal silicide nanowires over a mesoscopic area on Si(110)-16×2 surface. Three perfectly-ordered parallel arrays of atomically-precise Gd-silicide nanowires, Ce-silicide nanowires, and Er-silicide nanowires are presented to demonstrate the versatility of this novel approach. These massively parallel rare-earth silicide nanowire

arrays were self-organized with widths and pitches (center-to-center distances) as small as 4~5 nm and 6~8 nm, respectively, and lengths exceeding 1 μm, which were achieved through the heteroepitaxial growth of rare-earth metal silicides along the periodic terraces of the Si(110)-16×2 surface. The ability to form such large-area, highly-ordered parallel arrays of epitaxial rare-earth metal silicide nanowires on the Si(110) nanotemplate represents a simple step towards the bottom-up nanofabrication of high-density, well-defined interconnections and functional nanowire-based CMOS nanodevices in a straightforward, cost-effective and high-throughput process. As they have the advantage of easy integration into the existing silicon-based integrated-circuit technology, we believe that our developed large-scale self-organization of epitaxial rare-earth metal silicide nanowire arrays on Si(110)-16×2 surface will be an important Si-compatible nanofabrication process for highly-integrated, well-defined parallel active nanoarchitectures with diverse functions over mesoscopic areas, which could be used to realize the future innovations in Si-based nanoelectronics.

5. Acknowledgements

This work is financially supported by the National Science Council of Taiwan under Grant Nos. 97-2738-M-415-001 and 97-2112-M-415-003-MY3.

6. References

Agarawal, R. (2008). Heterointerfaces in Semiconductor Nanowires. *Small*, Vol. 4, No. 11, (April 2008), pp. 1872-1893, ISSN 1613-6829.

An, T.; Yoshimura, M.; Ono, I. & Ueda, K. (2000). Elemental Structure in Si(110)-''16x2'' Revealed by Scanning Tunneling Microscopy. *Physical Review B*, Vol. 61, No. 4 (January 2000), pp. 3006-3011, ISSN 1098-0121.

Castrucci, P.; Yubero, F. ; Vicentin, F. C.; Vogel, J. & Sacchi, M. (1995). Surface Crystal Field at The Er/Si(111) Interface Studied by Soft-X-Ray Linear Dichroism. *Physical Review B*, Vol. 52, No. 19, (November 1995), pp. 14035–14039, ISSN 1098-0121.

Chen, Y.; Ohlberg, D. A. A.; Medeiros-Ribeiro, G.; Chang, Y. A. & Williams, R. S. (2000). Self-Assembled Growth of Epitaxial Erbium Disilicide Nanowires on Silicon(001). *Applied Physics Letters*, Vol. 76, No. 26, (June 2000), pp. 4004-4006, ISSN 0003-6951.

Chen, Y.; Ohlberg, D. A. A. &Williams, R. S. (2002). Nanowires of Four Epitaxial Hexagonal Silicides Grown on Si(001). *Journal of Applied Physics*, Vol. 91, No. 5, (March 2002), pp. 3213-3218, ISSN 0021-8979, ISSN 0021-8979.

Cheng, W.; Teramoto, A.; Hirayama, M.; Sugawa, S. & Ohmi, T. (2006). Impact of Improved High-Performance Si(110)-Oriented Metal–Oxide–Semiconductor Field-Effect Transistors using Accumulation-Mode Fully Depleted Silicon-on-Insulator Devices. *Japanese Journal of Applied Physics*, Vol. 45, No. 48, (April 2006), pp. 3110-3116, ISSN 0021-4922.

Eames, C.; Probert, M. I. J. & Tear, S. P. (2010). The Structure and Growth Direction of Rare Earth Silicide Nanowires on Si(100). *Applied Physics Letters*, Vol. 96, No. 24, (June 2010), pp. 241903, ISSN 0003-6951.

Gambardella, P.; Dallmeyer, A.; Maiti, K.; Malagoli, M. C., Eberhardt, W.; Kern, K. & Carbone, C. (2002). Ferromagnetism in One-Dimensional Monatomicmetal Chains. *Nature*, Vol. 416, (March 2002), pp. 301-303, ISSN 0028-0836.

Hogg, S. M.; Vantomme, A. & Wu, M. F. (2002). Growth and Electrical Characterization of $GdSi_{1.7}$ Epilayers Formed by Channeled Ion Beam Synthesis. *Journal of Applied Physics*, Vol. 91, No. 6, (March 2002), pp. 3664-3668, ISSN 0021-8979.

He, Z.; Smith, D. J. & Bennett, P. A. (2004). Endotaxial Silicide Nanowires. *Physical Review Letters*, Vol. 93, No. 25, (December 2004), pp. 256102, ISSN 0031-9007.

Hong, I.-H.; Yen, S.-C. & Lin, F.-S. (2009). Two-Dimensional Self-Organization of an Ordered Au Silicide Nanowire Network on a Si(110)-16×2 Surface. *Small*, Vol. 5, pp. 1855–1861, ISSN 1613-6829.

Hong, I.-H.; Liao, Y.-C. & Yen, S.-C. (2009). Self-Organization of a Highly Integrated Silicon Nanowire Network on a Si(110)-16×2 Surface by Controlling Domain Growth. *Advanced Functional Materials*, Vol. 19, (November 2009), pp. 3389-3395, ISSN 161-3028.

Hong, I.-H.; Tsai, Y.-F. & Chen, T.-M. (2011). Self-Organization of Mesoscopically Ordered Parallel Gd-Silicide Nanowire Arrays on a Si(110)-16×2 Surface: A Massively Parallel Active Architecture. *Applied Physics Letters*, Vol. 98, No. 19, (May 2011), pp. 193118, ISSN 0003-6951.

Hong, I.-H. (2011). Self-Organization of Two-dimensional Highly-Regular Nanowire Meshes on Si(110)-16×2 Surface, Nova Science, *Mesh Networks*, to be published. ISBN 978-1-62100-150-8

Hong, I.-H.; Y.-C. Liao & Tsai, Y.-F. Electronic Structure of Strongly-Correlated Ce-Silicide Nanowires Self-Organized on Si(110)-16×2 Surface: One-Dimensional Mott-Hubbard Insulating State. Submitted to *Physical Review B*, ISSN 1098-0121.

Iancu, V.; Kent, P. R. C.; Zeng, C. G.; Weitering, H. H. (2009). Structure of YSi_2 Nanowires from Scanning Tunneling Spectroscopy and First Principles. *Applied Physics Letters*, Vol. 95, No. 12, (September 2009), pp. 123107, ISSN 0003-6951.

Lee, D. & Kim, S. (2003). Formation of Hexagonal Gd Disilicide Nanowires on Si(100). *Applied Physics Letters*, Vol. 82, No. 16, (April 2003), pp. 2619-2621, ISSN 0003-6951.

Lee, D.; Lim, D. K.; Bae, S. S.; Kim, S.; Ragan, R.; Ohlberg, D. A. A.; Chen, Y. & Williams, R. S. (2006). Unidirectional Hexagonal Rare-Earth Disilicide Nanowires on Vicinal Si(100)-2×1. *Applied Physics A: Materials Science & Processing*, Vol. 80, No. 6, (March 2005), pp. 1311–1313, ISSN 0947-8396.

Liang, S.; Islam, R.; Smith, D. J.; Bennett, P. A.; O'Brien, J. R. & Taylor, B. (2006). Magnetic iron silicide nanowires on Si(110). *Applied Physics Letters*, Vol. 88, No. 11, (March 2006), pp. 113111, ISSN 0003-6951.

Liu, B. Z. & Nogami, J. (2003). Growth of Parallel Rare-Earth Silicide Nanowire Arrays on Vicinal Si(001). *Nanotechnology*, Vol. 14, (June 2003), pp. 873–877, ISSN 0957-4484.

Liu, B. Z. & Nogami, J. (2003). A Scanning Tunneling Microscopy Study of Dysprosium Silicide Nanowire Growth on Si(001). *Journal of Applied Physics*, Vol. 93, No. 1, (January 2003), pp. 593-599, ISSN 0021-8979.

Lu, W. & Lieber, C. M. (2007). Nanoelectronics from The Bottom Up. *Nature Materials*, Vol. 6, (November 2007), pp. 841-850, ISSN 1476-1122.

McChesney, J. L.; Kirakosian, A.; Bennewitz, R.; Crain, J. N.; Lin, J.-L. & Himpsel, F. J. (2002). Gd Disilicide Nanowires Attached to Si(111) Steps. *Nanotechnology*, Vol. 13, (July 2002), pp. 545–547, ISSN 0957-4484.

Malterre, D.; Grioni, M.; Weibel, P.; Dardel, B. & Baer, Y. (1993). Correlation between The Kondo Temperature and The Photoemission Spectral Function in The $CeSi_x$ ($1.6 \leq x \leq 2$) System. *Physical Review B*, Vol. 48, No. 14, (October 1993), pp. 10599, ISSN 1098-0121.

Melosh, N. A. Boukai, A.; Diana, F.; Gerardot, B.; Badolato, A.; Petroff, P. M.; & Heath, J. R. (2003). Ultrahigh-Density Nanowire Lattices and Circuits. *Science*, Vol. 300, (April 2003), pp. 112-115, ISSN 0036-8075.

Mimura, K.; Noguchi, S.; Suzuki, M.; Higashiguchi, M.; Shimada, K.; Ichikawa, K.; Taguchi, Y.; Namatame, H.; Taniguchi, M. & Aita, O. (2005). Temperature Dependence of High-Resolution Resonant Photoemission Spectra of CeSi. *Journal of Electron Spectroscopy and Related Phenomena*. Vol. 144-147, (June 2005), pp. 715, ISSN 0368-2048.

Mizuno, T.; Sugiyama, N.; Tezuka, T.; Moriyama, Y.; Nakaharai, S. & Takagi, S.-I. (2005). [110]-surface strained-SOI CMOS devices. *IEEE Transaction on Electron Devices*, Vol. 52, No. 3, (March 2005), pp. 367-374, ISSN 0018-9383.

Münzenberg, M.; Felsch, W. & Schaaf, P. (2007). Tuning the *4f* State Occupancy of Ce in Highly Correlated CeSi/Fe Multilayers: An X-Ray Absorption Spectroscopy Study. *Physical Review B*, Vol. 76, No. 1, (July 2007) pp. 014427, ISSN 1098-0121.

Nogami, J.; Liu, B. Z.; Katkov, M. V.; Ohbuch, C. & Birge, N. O. (2001). Self-Assembled Rare-Earth Silicide Nanowires on Si(001). *Physical Review B*, Vol. 63, No. 23, (May 2001), pp. 233305, ISSN 1098-0121.

Ohbuchi, C. & Nogami, J. (2002). Holmium Growth on Si(001): Surface Reconstructions and Nanowire Formation. *Physical Review B*, Vol. 66, No. 16, (October 2002), pp. 165323, ISSN 1098-0121.

Padova, P.D.; Quaresima, C.; Perfetti, P.; Olivieri, B.; Leandri, C.; Aufray, B.; Vizzini, S. & Lay, G. L. (2008). Growth of Straight, Atomically Perfect, Highly Metallic Silicon Nanowires with Chiral Asymmetry. *Nano Letters*, Vol. 8, No. 1, (November 2007), pp. 271-275, ISSN 1530-6984.

Pierre, J.; Auffrettll, S.; Chroboczek, J. A. & Nguyen, T. T. A. (1994). Magnetotransport in the Rare Earth Silicides RSi_{2-x}, *Journal of Physics: Condensed Matter*, Vol. 6, No. 1, (January 1994), pp. 79-92, ISSN 0953-8984.

Pecharsky, V. K. & Gschneidner Jr., K. A. (2001). $Gd_5(Si_{1-x}Ge_x)_4$: An Extremum Material. *Advanced Materials*, Vol. 13, No. 9, (May 2001), pp. 683-686, ISSN 1521-4095.

Preinesberger, C.; Pruskil, G.; Becker, S. K.; Dähnea, M.; Vyalikh, D. V.; Molodtsov, S. L.; Laubschat, C. & Schiller, F. (2005). Structure and Electronic Properties of Dysprosium-Silicide Nanowires on Vicinal Si(001). *Applied Physics Letters*, Vol. 87, No. 8, (August 2005), pp. 083107, ISSN 0003-6951.

Qiu, D.; Zhang, M.-X. & Kelly & P. M. (2009). Crystallography of Self-Assembled $DySi_2$ Nanowires on Si Substrate. *Applied Physics Letters*, Vol.94, No. 8, (February 2009), pp. 083105, ISSN 0003-6951.

Sahaf, H.; Masson, L.; Léandri, C.; Aufray, B.; Lay, G. L. & Ronci F. (2007). Formation of A One-Dimensional Grating at the Molecular Scale by Self-Assembly of Straight Silicon Nanowires. *Applied Physics Letters*, Vol. 90, No. 26, (June 2007), pp. 263110, ISSN 0003-6951.

Segovia, P.; Purdie, D.; Hengsberger, M. & Baer, Y. (1999). Observation of Spin and Charge Collective Modes in One-Dimensional Metallic Chains. *Nature*, Vol. 402, (December 1999), pp. 504-507, ISSN 0028-0836.

Shaheen, S. A. & Mendoza, W. A. (1999). Origin of Multiple Magnetic Transitions in $CeSi_x$ Systems. *Physical Review B*, Vol. 60, No. 13, (October 1999), pp. 9501-9505, ISSN 1098-0121.

Shchukin, V. A. & Bimberg, D. (1999). Spontaneous Ordering of Nanostructures on Crystal Surfaces. *Reviews of Modern Physics*, Vol.*71*, No. 4, (July 1999), pp. 1125-1171, ISSN 0034-6861.

Smith, J. S.; Zan, J. A.; Lin, C. L. & Li, J. (2005). Electric, Thermal, and Magnetic Properties of $CeSi_x$ with $1.57<x\leq2.0$. *Journal of Applied Physics*, Vol. 97, No. 10, (May 2005), pp. 10A905, ISSN 0021-8979.

Snijders, P. C. & Weitering, H. H. (2010). *Colloquium*: Electronic instabilities in self-assembled atom wires. *Reviews of Modern Physics*, Vol. 82, No. 1, (January 2010), pp. 307-329, ISSN 0034-6861.

Soukiassian, P.; Semond, F.; Mayne, A. & Dujardin, G. (1997). Highly Stable Si Atomic Line Formation on the β-SiC(100) Surface. *Physical Review Letters*, Vol. 79, No. 13, (September 1997), pp. 2498-2501, ISSN 0031-9007.

Stekolnikov, A. A.; Furthmüller, J. & Bechstedt, F. (2004). Long-Range Surface Reconstruction: Si(110)-16×2. *Physical Review Letters*, Vol. 93, No. 13, pp. 136104, ISSN 0031-9007.

Yamamoto, Y.; Sueyoshi, Sato, T. T. & Iwatsuki, M. (2000). High-Temperature Scanning Tunneling Microscopy Study of the '16×2'⇔(1×1) Phase Transition on an Si(110) Surface. *Surface Science*, Vol. 466, (August 2000), pp. 183-188, ISSN 0036-8075.

Yang, M.; Chan, W. C.; Shi, L.; Fried, D. M.; Stathis, J. H.; Chou, A. I.; Gusev, E.; Ott, J. A.; Burns, L. E.; Fischetti, M. V. & Ieong, M. (2006). Hybrid-Orientation Technology (HOT): Opportunities and Challenges. *IEEE Transaction on Electron Devices*, Vol. 53, No. 5, (May 2006), pp. 965-978, ISSN 0018-9383.

Ye, G.; Crimp, M. A. & Nogami, J. (2009). Self-Assembled Gd Silicide Nanostructures Grown on Si(001). *Journal of Applied Physics*, Vol. 105, No. 10, (May 2009), pp. 104304, ISSN 0021-8979.

Yeom, H. W.; Kim, Y. K.; Lee, E. Y.; Ryang, K.-D.; Kang, & P. G. (2005), Robust One-Dimensional Metallic Band Structure of Silicide Nanowires. *Physical Review Letters*, Vol. 95, No. 20, (November 2005), pp. 205504, ISSN 0031-9007.

Yokota, T.; Fujimura, N. & Ito, T. (2002). Effect of Substitutionally Dissolved Ce in Si on the Magnetic and Electric properties of Magnetic Semiconductor $Si_{1-x}Ce_x$ Films. *Applied Physics Letters*, Vol. 81, No. 21, (Noveber 2002), pp. 4023-4025, ISSN 0003-6951.

Zeng, C. G.; Kent, P. R .C.; Kim, T.-H.; Li, A.-P.; Weitering, H. H. (2008). Charge-Order Fluctuations in One-Dimensional Silicides. *Nature Materials*, Vol. 7, (July 2008), pp. 539-542, ISSN 1476-1122.

Zhirnov, V. V. & Herr, D. J. C. (2001). New Frontiers: Self-Assembly and Nanoelectronics. *Computer*, Vol. 34, No. 1, (January 2001), pp. 34-43, ISSN 0018-9162.

Zhou, W.; Zhu, Y. Ji T.; Hou, X. & Cai, Q. (2006). Formation and Evolution of Erbium Silicide Nanowires on Vicinal and Flat Si(001). *Nanotechnology*, Vol. 17, (January 2006), pp. 852–858, ISSN 0957-4484.

Žutić, I. (2006). Gadolinium Makes Good Spin Contacts. *Nature Materials*, Vol. 5, (October 2006), pp. 771-772, ISSN 1476-1122.

Wanke, M.; Löser, K.; Pruskil, G. & Dähne, M. (2009). Structural and Electronic Properties of Rare Earth Silicide Nanowires on Si(557). *Physical Review B*, Vol. 79, No. 15, (April 2009), pp. 155428, ISSN 1098-0121.

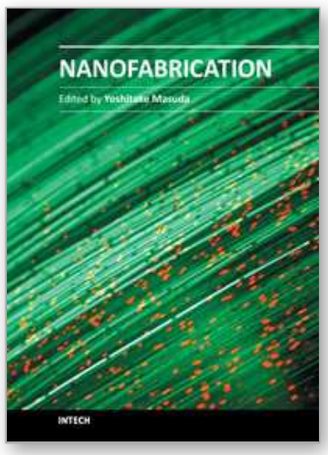

Nanofabrication

Edited by Dr. Yoshitake Masuda

ISBN 978-953-307-912-7
Hard cover, 354 pages
Publisher InTech
Published online 22, December, 2011
Published in print edition December, 2011

We face many challenges in the 21st century, such as sustainably meeting the world's growing demand for energy and consumer goods. I believe that new developments in science and technology will help solve many of these problems. Nanofabrication is one of the keys to the development of novel materials, devices and systems. Precise control of nanomaterials, nanostructures, nanodevices and their performances is essential for future innovations in technology. The book "Nanofabrication" provides the latest research developments in nanofabrication of organic and inorganic materials, biomaterials and hybrid materials. I hope that "Nanofabrication" will contribute to creating a brighter future for the next generation.

How to reference

In order to correctly reference this scholarly work, feel free to copy and paste the following:

Ie-Hong Hong (2011). Self-Organization of Mesoscopically-Ordered Parallel Rare-Eath Silicide Nanowire Arrays on Si(110)-16×2 Surface, Nanofabrication, Dr. Yoshitake Masuda (Ed.), ISBN: 978-953-307-912-7, InTech, Available from: http://www.intechopen.com/books/nanofabrication/self-organization-of-mesoscopically-ordered-parallel-rare-eath-silicide-nanowire-arrays-on-si-110-16

INTECH
open science | open minds

InTech Europe
University Campus STeP Ri
Slavka Krautzeka 83/A
51000 Rijeka, Croatia
Phone: +385 (51) 770 447
Fax: +385 (51) 686 166
www.intechopen.com

InTech China
Unit 405, Office Block, Hotel Equatorial Shanghai
No.65, Yan An Road (West), Shanghai, 200040, China
中国上海市延安西路65号上海国际贵都大饭店办公楼405单元
Phone: +86-21-62489820
Fax: +86-21-62489821

IntechOpen